Characterization of Calcined and Reduced Multi-Component Co−Ni−Mg−Al-Layered Double Hydroxides

Didier Tichit,*[a] Solange Ribet,[a] and Bernard Coq[a]

Keywords: Clays / Cobalt / Nickel / Reductions / Spinel phases

Several Co–Ni–Mg–Al-layered double hydroxides (LDH) have been synthesized by coprecipitation at constant pH = 9. All samples present well crystallized, layered structures, no excess phases were detected by X-ray diffraction, and the lattice *a* parameter followed the Vegard correlation. The cations thus belong to the same, brucite-like, lattice. Calcined samples exhibit XRD patterns of the crystallographic phase preferentially adopted by the major cation in the LDH: i.e., a mixed oxide of the rock salt type in the case of Ni or Mg, and a spinel-like structure for Co. Surface areas reached maximum values in the range of 200–300 m^2g^{-1} after calcination at 573 K. They were stabilized with increasing Ni or Mg content, as higher amounts of mixed oxide phase were formed. Programmed temperature reduction showed two domains of H_2 consumption, assigned to reduction of $Co_{3-x}Ni_xO_4$ species below 720 K, and to NiMg(Al)O and $Co_{3-x-y}Ni_xMg_yAlO_6$, of rock salt type and spinel-like structures respectively, above this temperature. These assignments are in agreement with the XRD patterns and show that Ni and Co are associated in the same crystallographic phases.

Introduction

Layered double hydroxides (LDHs) or anionic clays of the general formula $[M_{1-x}^{2+}M_x^{3+}(OH)_2]^{x+}[A^{m-}]_{x/m}\cdot n\,H_2O$ are increasingly used as precursors of catalysts with varying divalent and trivalent cations in their layers.[1] These two cations are distributed inside brucite-like sheets in an octahedral environment. The structure is based on the stacking of these positively charged layers, with hydrated compensating anions in the interlamellar domain.[1,2] Interest in LDHs is undoubtedly increasing because not only two but, more frequently, several cations may be accommodated in the structure, thus leading to a wide variety of multi-component catalyst precursors. Therefore, the intrinsic properties of the resulting catalysts − like acido-basicity and hydrogenating or oxidizing capabilities − might be tuned through the nature and the relative quantities of the cations and the activation conditions. We previously reported that highly active and selective catalysts for the hydrogenation of acetonitrile into ethylamine were obtained when using Co/Ni/Mg/Al LDH precursors.[3] Improvements of these catalysts, which require Ni or Co metals deposited on poorly acidic supports, resulted from adjustment of the Mg content and of alloying Ni, the active metal, with Co.[3,4]

This work is aimed at the study of the synthesis and activation of quaternary Co−Ni−Mg−Al LDHs. Their decomposition has been followed under oxidizing and reducing atmospheres. Special attention has been paid to temperature programmed reduction (TPR) experiments to support XRD in the identification of the nature of phases present in the precursor.

[a] Laboratoire de Matériaux Catalytiques et Catalyse en Chimie Organique, CNRS, UMR 5618, E.N.S.C.M 8,
Rue Ecole Normale, 34296 Montpellier Cedex 5, France
Fax: (internat.) + 33-4/67144349
E-mail: tichit@cit.enscm.fr

Results

Synthesis of the LDH Precursors

Cationic contents of the synthesis solutions and formula of the solids as deduced from their chemical analysis are given in Table 1. It is assumed that all cobalt is in the form of Co^{2+}. The water content is evaluated from TG analysis. As can be seen, Co and Ni content in the layers is close to the corresponding levels in solution. In contrast, the Mg content is always slightly lower than expected. This behavior is in accordance with the respective precipitation pHs of Co, Ni, and Mg in their hydroxide forms, occurring from pH = 9 for the first two elements, but at pH above 10 for the last.

The slight variations described above obviously dictate that the layer charges of the different samples are not strictly identical, since $x = Al^{3+}/(\Sigma M^{2+}+Al^{3+})$ is in the range of 0.25−0.28.

Both nitrate and carbonate anions are present in the structures, always with an excess of anionic charge. This probably results from the presence not only of CO_3^{2-} but also of HCO_3^-, very often formed at pH ≈ 9. The presence of CO_3^{2-} is consistent with contamination by air during synthesis.

XRD profiles of the samples, dried at 353 K, are reported in Figure 1. They show that a single hydrotalcite-like phase is present in all cases, with several (00*l*) reflections. The (003) reflection is usually sharp; in contrast, the (006) and higher reflections are broad in the samples containing Co, Ni, and Mg concomitantly. Such features provide evidence of structures poorly ordered along the *c* axis.

  1434−1948/01/0202−0539 $ 17.50+.50/0

Table 1. Proportion of cations in the synthesis solutions and elemental composition of the various Co−Ni−Mg−Al samples

Samples	Synthesis solutions ($M^{2+}/\Sigma M^{n+}$)				Composition of solids	*a* (nm)	*c* (nm)
	Co^{2+}	Ni^{2+}	Mg^{2+}	Al^{3+}			
Co(3)Al	0.75	0.00	0.00	0.25	$[Co_{0.75}Al_{0.25}(OH)_2](CO_3^{2-})_{0.07}(NO_3^-)_{0.12}$, 0.6 H_2O	0.308(8)	2.335(0)
Co(2)Mg(1)Al	0.50	0.00	0.25	0.25	$[Co_{0.53}Mg_{0.18}Al_{0.28}(OH)_2](CO_3^{2-})_{0.07}(NO_3^-)_{0.14}$, 0.6 H_2O	0.307(4)	2.402(2)
Co(1.5)Ni(0.5)Mg(1)Al	0.37	0.12	0.25	0.25	$[Co_{0.40}Ni_{0.13}Mg_{0.19}Al_{0.28}(OH)_2](CO_3^{2-})_{0.05}(NO_3^-)_{0.23}$, 0.6 H_2O	0.306(4)	2.511(1)
Co(1)Ni(1)Mg(1)Al	0.25	0.25	0.25	0.25	$[Co_{0.27}Ni_{0.26}Mg_{0.21}Al_{0.26}(OH)_2](CO_3^{2-})_{0.04}(NO_3^-)_{0.19}$, 0.6 H_2O	0.305(7)	2.511(1)
Co(0.5)Ni(1.5)Mg(1)Al	0.12	0.37	0.25	0.25	$[Co_{0.14}Ni_{0.38}Mg_{0.21}Al_{0.28}(OH)_2](CO_3^{2-})_{0.07}(NO_3^-)_{0.19}$, 0.6 H_2O	0.305(0)	2.455(4)
Ni(2)Mg(1)Al	0.00	0.50	0.25	0.25	$[Ni_{0.53}Mg_{0.19}Al_{0.28}(OH)_2](CO_3^{2-})_{0.05}(NO_3^-)_{0.22}$, 0.6 H_2O	0.304(1)	2.520(6)
Co(1.5)Ni(1.5)Al	0.38	0.37	0.00	0.25	$[Co_{0.36}Ni_{0.36}Al_{0.28}(OH)_2](CO_3^{2-})_{0.04}(NO_3^-)_{0.23}$, 0.5 H_2O	0.305(3)	2.620(0)
Co(0.8)Ni(0.8)Mg(1.4)Al	0.30	0.30	0.15	0.25	$[Co_{0.32}Ni_{0.33}Mg_{0.10}Al_{0.26}(OH)_2](CO_3^{2-})_{0.12}(NO_3^-)_{0.21}$, 0.6 H_2O	0.305(9)	2.428(5)
Co(1.2)Ni(1.2)Mg(0.6)Al	0.20	0.20	0.35	0.25	$[Co_{0.20}Ni_{0.20}Mg_{0.31}Al_{0.28}(OH)_2](CO_3^{2-})_{0.10}(NO_3^-)_{0.12}$, 0.6 H_2O	0.305(9)	2.530(2)

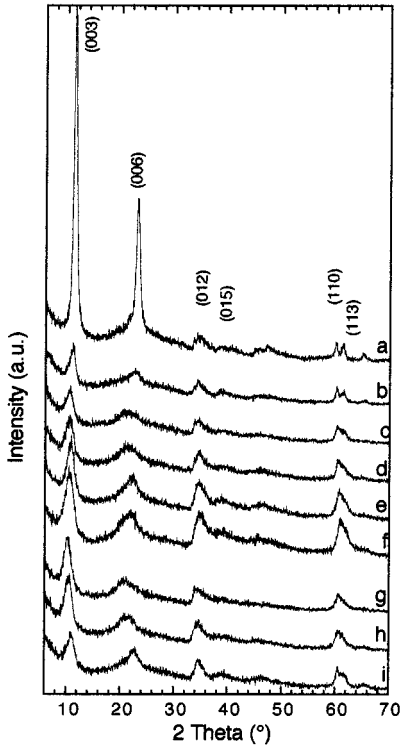

Figure 1. X-ray diffraction patterns of the different samples: (a): Co(3)Al, (b): Co(2)Mg(1)Al, (c): Co(1.5)Ni(0.5)Mg(1)Al, (d): Co(1)Ni(1)Mg(1)Al, (e): Co(0.5)Ni(1.5)Mg(1)Al, (f): Ni(2) Mg(1)Al, (g): Co(1.5)Ni(1.5)Al, (h): Co(1.2)Ni(1.2)Mg(0.6)Al, (i): Co(0.8)Ni(0.8)Mg(1.4)Al

Some peculiar characteristics can otherwise be quoted:

(1) for the series of materials of identical Mg content ($Mg^{2+}/\Sigma M^{2+}$ = 1:3), the (003) and (006) peaks become progressively sharper and the (11*l*) peaks vanish as the Ni content increases. Stacking order between the layers thus increases at the expense of that within the layers.

(2) Mg content has a lesser influence on the shape of the XRD patterns. Its smaller ionic size (0.065 nm) compared to Ni (0.069 nm) or Co (0.074 nm) induces less distortion of the layers.

Therefore, the orders along the *a* and *c* crystallographic directions of the multi-component LDHs mainly depend on their Co and Ni content. Accordingly, the lattice *a* parameter follows the Vegard correlation with the Co or Ni content (Figure 2), but is independent of the Mg content (Table 1). No clear relationship exists between the lattice *c* parameter and Co and Ni content, while a small decrease is noted with Mg content at similar Ni/(Co+Ni) ratio (Table 1). This could not reasonably be assigned to a variation of the layer charge. To sum up, the existence of a unique (003) line and the evolution of the lattice *a* parameter, in agreement with the Vegard correlation, show that all cations belong to the same brucite-like lattice class. Moreover, a low crystallinity of the samples is in line with this assumption, if one considers that up to four cations are accommodated in the layers.

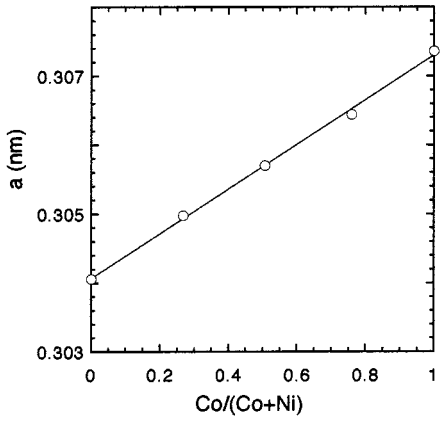

Figure 2. Variation of the lattice *a* parameter of the Co−Ni−Mg−Al samples as a function of Co/(Co+Ni) ratio for $Mg^{2+}/\Sigma M^{2+}$ = 1:3

Results of TG-DTG analysis are given in Table 2. Mass losses occur in two steps up to 973 K, as classically found with Mg−Al and M−Mg−Al samples (M = Ni, Co).[5−10] The low-temperature weight loss originates from the removal of water molecules in the interlayer space and weakly bonded CO_3^{2-} species.[5,7] Dehydroxylation of the layers with concomitant H_2O release, and decomposition of the anions result in the weight loss at 540−600 K. Total weight losses, in the range of 33−39 wt%, increase significantly with Mg content. This is due to the greater water release at ca 350 K in the Mg-containing samples, owing to the higher hydration ability of Mg compared to Ni and Co.

The first peak is at about 393 K in all cases, while there is a systematic shift of the second peak from 543 to 623 K when the Ni/(Co+Ni) molar ratio increases with similar Mg content.

Table 2. Weight losses and temperatures of maximum rates in the thermogravimetric analysis of the various samples

Samples	Total weight loss (%)	1st weight loss T_1 (K)	wt (%)	2nd weight loss T_2 (K)	wt (%)
Co(3)Al	28	463	10	503	18
Co(2)Mg(1)Al	35	393	11	543	24
Co(1.5)Ni(0.5)Mg(1)Al	37	393	10	563	27
Co(1)Ni(1)Mg(1)Al	37	393	10	583	27
Co(0.5)Ni(1.5)Mg(1)Al	38	403	11	603	27
Ni(2)Mg(1)Al	39	383	10	623	29
Co(1.5)Ni(1.5)Al	33	383	8	583	25
Co(1.2)Ni(1.2)Mg(0.6)Al	35	393	9	583	26
Co(0.8)Ni(0.8)Mg(1.4)Al	38	383	13	583	25

Calcination of the LDH Precursors

Calcination of LDH precursors leads to one or several phases. Their number and nature depend on the cations involved in the structure and on the temperature. However, some general tendencies can be expected, considering that below 1100 K, Ni and Mg probably form mixed oxides of NiO and MgO type on the one hand,[9,11,12] while, on the other hand, Co easily forms spinel-like structures.[7,8] The results from TG experiments prompted us to study the samples calcined at 573 and 773 K, since the main structural transformations of LDHs occur in this temperature range.

XRD patterns of the materials calcined at 773 K (Figure 3) look very different, depending on cation composition. For a given sample, the only change observed when the calcination temperature increases from 573 to 773 K is a better crystallinity.

For Ni(2)Mg(1)Al, the (111), (200), and (220) reflections of the NiO-like structure are recorded at 0.2422, 0.2087, and 0.1473 nm. These values are slightly shifted toward lower values than in the pure rock salt type single oxide (04-0835 ICDD data file), due to the presence of smaller ionic radius Al^{3+} within the lattice. For Co(2)Mg(1)Al, reflections at 0.4679, 0.2875, 0.2448, 0.2025, 0.1647, 0.1561, and 0.1432 nm can be assigned to the (111), (220), (311), (400), (422), (511), and (440) planes, respectively, of $CoAl_2O_4$ or Co_3O_4 spinel phases, which are indistinguishable. Such an assignment assumes that Co_3O_4 is thermodyamically more stable under air than CoO.[13] Moving now to quaternary LDHs, the case of Co(1)Ni(1)Mg(1)Al is archetypal, since the most intense peaks both of the rock salt type and of the spinel-like phases are detected. Actually, calcined LDHs exhibit XRD patterns of the crystallographic phases preferentially adopted by the major cation in the structure. Accordingly, Co(0.5)Ni(1.5)Mg(1)Al, Co(0.8)Ni(0.8)Mg(1.4)Al, on the one hand, and Co(1.5)-Ni(0.5)Mg(1)Al, Co(1.2)Ni(1.2)Mg(0.6)Al, on the other hand, present profiles of mixed oxide and spinel-like phases, respectively.

Several relevant features concern the textural properties of the different samples, either non-calcined, or calcined at 573 and 773 K (Table 3). Specific surface areas are generally low, from 20 to 90 m^2g^{-1} for the non-calcined samples, only outgassed at 473 K. This is due to still remaining compensating anions, as shown by the temperatures of the second

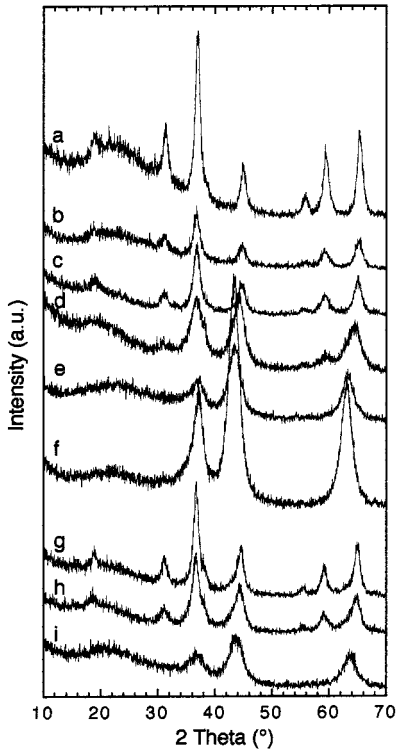

Figure 3. X-ray diffraction patterns of the samples calcined at 773 K: (a): Co(3)Al, (b): Co(2)Mg(1)Al, (c): Co(1.5)Ni-(0.5)Mg(1)Al, (d): Co(1)Ni(1)Mg(1)Al, (e): Co(0.5)Ni(1.5)-Mg(1)Al, (f): Ni(2)Mg(1)Al, (g): Co(1.5)Ni(1.5)Al, (h): Co(1.2)Ni-(1.2)Mg(0.6)Al, (i): Co(0.8)Ni(0.8)Mg(1.4)Al

DTG peaks in the range 540−620 K, except for Co(2)-Mg(1)Al. The adsorption isotherms of the calcined samples are of type II (Figure 4) and the full adsorption−desorption isotherms exhibit type H3 hysteresis loops. Nonetheless, although a hysteresis loop is observed, the isotherms are classified as type IIb (according to Rouquerol et al.[14]) rather than as type IV, because no plateau is observed at high P/P_0. Such adsorption−desorption isotherms are characteristic of aggregates of plate-like particles, classically found with clays. Specific surface areas go through maximum values after calcination at 573 K (Table 3). Their decrease above this temperature is in line with the enhancement of crystallinity shown by XRD. It should be pointed out that, after calcination at 773 K, the specific surface area is higher when Ni

Table 3. Specific surface areas and porous volumes of the various samples

Samples	non-calcined[a] S_{BET} (m^2g^{-1})	V_{por}[b] (cm^3g^{-1})	calcined 573 K S_{BET} (m^2g^{-1})	V_{por}[b] (cm^3g^{-1})	calcined 773 K S_{BET} (m^2g^{-1})	V_{por}[b] (cm^3g^{-1})
Co(3)Al	–	–	166	0.307	145	0.330
Co(2)Mg(1)Al	174	0.175	230	0.309	149	0.236
Co(1.5)Ni(0.5)Mg(1)Al	17	0.030	209	0.199	163	0.201
Co(1)Ni(1)Mg(1)Al	20	0.042	235	0.193	199	0.231
Co(0.5)Ni(1.5)Mg(1)Al	30	0.058	254	0.266	204	0.293
Ni(2)Mg(1)Al	20	0.060	251	0.211	192	0.237
Co(1.5)Ni(1.5)Al	13	0.020	201	0.169	144	0.173
Co(1.2)Ni(1.2)Mg(0.6)Al	15	0.264	234	0.187	127	0.175
Co(0.8)Ni(0.8)Mg(1.4)Al	96	0.023	296	0.435	270	0.489

[a] Outgassed at 473 K. – [b] Porous volume determined from N_2 uptake at $P/P_0 = 0.95$.

progressively substitutes for Co in samples of similar Mg content, or when Mg content increases in samples of similar Co/(Co+Ni) ratio. Indeed well crystallized spinel-like phases result in lower specific surface areas than rock salt-like structures. Microporosity increases with Mg content: i.e., when mixed oxide becomes the major phase. A limited degree of microporosity sometimes appears even though a type II isotherm is found.[14] A slightly higher microporous volume in Mg-containing samples than in Ni-containing counterparts is in agreement with the results reported for Mg(Al)O and Ni(Al)O mixed oxides.[10]

Reduction of the Calcined Materials

TPRs have been performed on the calcined samples. Some profiles are presented in Figure 5, and H_2 uptakes listed in Table 4. Two distinct domains of H_2 consumption – at low (LT) and high (HT) temperature – always appear as previously reported for Co–Al and Co–Mg–Al LDHs.[3] In the LT domain, one can observe a shoulder at about 473 K, then a highly intense peak with its maximum increasing with Co content, going from 533 K for Co(0.5)Ni(1.5)Mg(1)Al to 638 K for Co(2)Mg(1)Al. Both peaks may be assigned to the reduction of Co species, since they are not detected on Ni(2)Mg(1)Al; moreover, their intensities regularly increase with the Co content of Co–Ni–Mg–Al LDHs. For Co–Al and Co–Mg–Al samples, the shoulder at about 473 K in the LT domain was not identified so unequivocally, and was assigned to reduction of Co_3O_4.[6] These propositions will be discussed more extensively later for Co–Ni–Mg–Al LDHs.

In the HT domain, TPR profiles of the ternary LDHs containing only one reducible cation are very distinct. They differ in a narrow and intense peak extending over 100 K

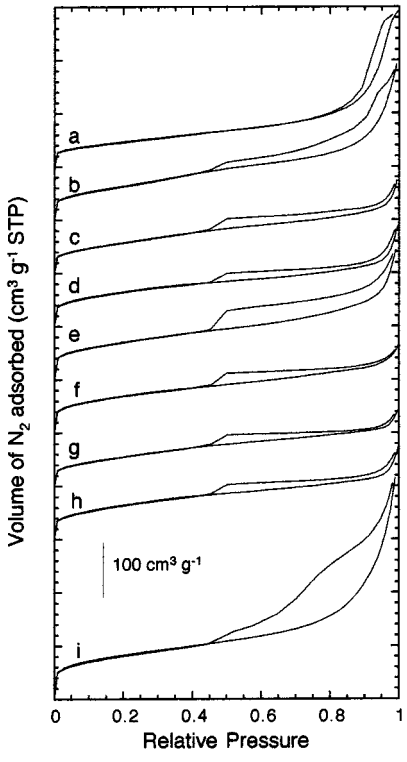

Figure 4. Nitrogen adsorption–desorption isotherms at 77 K of the samples calcined at 573 K: (a): Co(3)Al, (b): Co(2)Mg(1)Al, (c): Co(1.5)Ni(0.5)Mg(1)Al, (d): Co(1)Ni(1)Mg(1)Al, (e): Co(0.5)-Ni(1.5)Mg(1)Al, (f): Ni(2)Mg(1)Al, (g): Co(1.5)Ni(1.5)Al, (h): Co(1.2)Ni(1.2)Mg(0.6)Al, (i): Co(0.8)Ni(0.8)Mg(1.4)Al

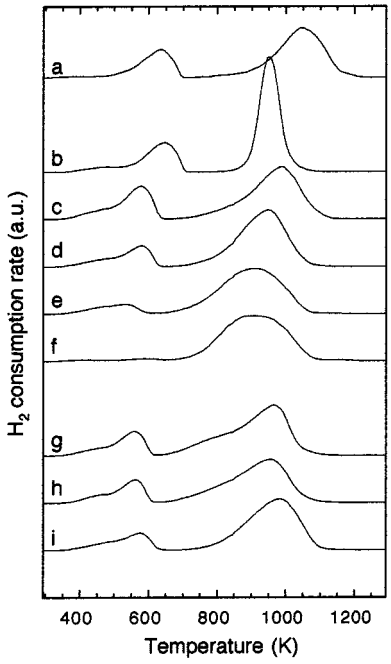

Figure 5. Temperature programmed reduction profiles of the samples calcined at 773 K: (a): Co(3)Al, (b): Co(2)Mg(1)Al, (c): Co(1.5)Ni(0.5)Mg(1)Al, (d): Co(1)Ni(1)Mg(1)Al, (e): Co(0.5)-Ni(1.5)Mg(1)Al, (f): Ni(2)Mg(1)Al, (g): Co(1.5)Ni(1.5)Al, (h): Co(1.2)Ni(1.2)Mg(0.6)Al, (i): Co(0.8)Ni(0.8)Mg(1.4)Al

Table 4. H_2 uptakes (H_2/Co+Ni), mol/mol) in TPR experiments

Samples	calcined at 623 K			calcined at 773 K		
	total	LT	HT	total	LT	HT
Co(3)Al	0.99	0.29	0.70	0.99	0.28	0.71
Co(2)Mg(1)Al	1.23	0.42	0.81	1.11	0.33	0.78
Co(1.5)Ni(0.5)Mg(1)Al	1.23	0.41	0.82	1.17	0.35	0.82
Co(1)Ni(1)Mg(1)Al	1.13	0.33	0.80	1.06	0.22	0.84
Co(0.5)Ni(1.5)Mg(1)Al	1.14	0.25	0.89	1.01	0.12	0.89
Ni(2)Mg(1)Al	1.07	0.15	0.92	0.93	0.00	0.93
Co(1.5)Ni(1.5)Al	1.22	0.31	0.91	1.11	0.24	0.87
Co(1.2)Ni(1.2)Mg(0.6)Al	1.30	0.38	0.92	1.01	0.23	0.78
Co(0.8)Ni(0.8)Mg(1.4)Al	1.23	0.41	0.82	1.04	0.20	0.84

for Co(2)Mg(1)Al, and a large and broad feature extending over 400 K for Ni(2)Mg(1)Al. For Co(1.5)Ni(1.5)Al, with two reducible cations, maxima at 820 and 960 K reflect the presence of Co and Ni reducible phases respectively.

Finally, in the quaternary LDHs, several remarks may be made concerning the influence of Co/(Co+Ni) ratio:

(1) The shape of the TPR peak moves progressively from that characteristic of Co(2)Mg(1)Al to that characteristic of Ni(2)Mg(1)Al upon Ni substitution.

(2) Compared to the Ni free sample [Co(2)Mg(1)Al], a shift of 30 K toward higher temperature is noted when Ni is introduced in low amount [Co(1.5)Ni(0.5)Mg(1)Al]; after that the temperature of maximum H_2 consumption rate is shifted toward lower values when the Ni content becomes higher.

(3) The temperatures of maximum H_2 consumption rates are rather insensitive to the Mg content.

(4) The TPR profiles of samples at identical Co and Ni content [Co/(Co+Ni) = 0.5] are not the simple averaging of those of Co(2)Mg(1)Al and Ni(2)Mg(1)Al samples.

This last remark demands a more detailed discussion, which is emphasized when looking carefully at the H_2 consumption values of samples calcined at 773 K (Table 4). For Co(2)Mg(1)Al, H_2 consumption in the LT and HT domains represents 30 and 70% of the total, respectively. The total H_2/Co molar ratio of 1.11 for this sample is thus consistent with the presence of Co^{3+} in Co_3O_4; this is normally reduced to Co^0 at low temperature, as proposed by Arnoldy and Moulijn.[13] In the TPR of Ni(2)Mg(1)Al, all H_2 was taken up above 600 K; this was previously assigned to NiO-type phase reduction to Ni^0 in similar materials.[5] On the basis of simple combination of the H_2 consumption values for Ni and Co, one might expect that the H_2 taken up in the LT and HT domains for Co(1.5)Ni(1.5)Al would be 15% and 85%, respectively. However, the actual distribution is 22% and 78%. This is a general behavioral pattern, and significantly higher values for H_2 consumption in the LT range persist when Mg is present and/or the Co/(Co+Ni) ratio modulated.

Discussion

The goal when preparing these LDHs was to develop new bimetallic hydrogenation catalyst precursors, particularly active and selective for the hydrogenation of acetonitrile into ethylamine.[3] In this respect it was of utmost importance to identify the kind of intimate vicinity and of interaction between Ni and Co at the different stages of catalyst elaboration. On that account, we will pay special attention in the following discussion to the nature of the phases obtained upon calcination and their evolution during TPR experiments.

As a first step, TG and XRD analysis of the "as-prepared" materials have shown that a unique LDH phase exists. This is, moreover, clearly highlighted in Figure 6, which shows a correlation appearing between the temperature of maximum weight loss from DTG plots (Table 2) and the *a* parameter (Table 1) for samples of various Co/(Co+Ni) ratios and similar Mg content. The temperature of anion decomposition derived from DTG plots reflects the strength of electrostatic interaction between the layers and the anions. When Ni is substituted for Co, the lattice *a* parameter decreases and the positive charges thus become more localized, enhancing the electrostatic attraction with the anions.

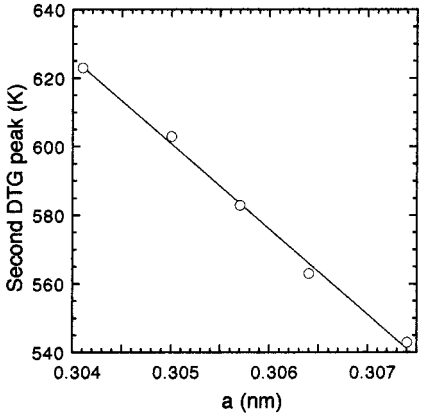

Figure 6. Correlation between the temperature of the second DTG peak and the *a* parameter for the Co−Ni−Mg−Al samples with $Mg^{2+}/\Sigma M^{2+}$ = 1:3

Upon calcination of LDH precursors, one obtains Ni- and Co-containing oxide phases of complex nature and composition. Co-containing LDHs give rise to a crystalline Co_3O_4 phase after calcination at 573 K. In the case of multi-component Co−Ni−Mg−Al LDHs, this behavior might be clarified by examination of the chemical compositions, XRD patterns, and reduction processes in TPR experiments. The reduction of calcined supported Ni catalysts has shown that the prevailing species belong to the NiO-type phase.[15−17]

In contrast, several studies on cobalt or cobalt-magnesium silica gels,[18,19] CoO/Al_2O_3,[13] or Co/SiO_2[20] catalysts reveal the complexity of the reduction process and the multiplicity of phases involved. For example, reduction of Co species, belonging to up to eight sub-phases, occurs within four different temperature domains for Co/Al_2O_3 materials.[13]

As far as the reduction processes in Co−Ni−Mg−Al LDHs are concerned, the main difficulties come from the multiplicity of possible occurring phases. A first remarkable

feature is that the shapes of the reduction profiles above 723 K are unchanged for Co−Mg−Al and Co−Ni−Mg-Al LDHs calcined at 573 or 773 K. This is consistent with the invariance in this temperature range of the crystalline phases detected by XRD. Hence, probably only weak diffusion of the cations is taking place during calcination or reduction processes.

We shall first discuss the reduction processes occurring in the LT domain (< 720 K). There is no peak of hydrogen consumption in the LT domain for the Co-free sample. On that account, the group of peaks appearing at LT for Co-containing materials must correspond to reduction of Co species. This peak was generally a broad feature arising from unresolved contributions. Compared to Co(3)Al, the reduction of Co is made easier in ternary or quaternary compounds containing Co and Ni. At variance with this, reduction of Co is more difficult in Co(2)Mg(1)Al than in Co(3)Al. The hydrogen consumption peak maxima at LT coincide with those generally found for reduction of bulk Co_3O_4[13] in the sequence $Co_3O_4 \rightarrow CoO \rightarrow Co$. Two reduction peaks have indeed been reported for bulk Co_3O_4, silica-supported Co catalysts[20] and promoted cobalt-Kieselguhr Fischer−Tropsch catalysts.[21] However, the reduction of Co_3O_4 to Co^0 on alumina-supported catalyst exhibits only one broad reduction peak,[13] which looks like that observed for reduction of Co(3)Al (Figure 5). The decrease of reducibility of Co upon addition of Mg can be discussed in parallel with the effect of MgO addition, which delayed the reduction of CoO in Kieselguhr-supported Co catalysts.[21] This behavior was ascribed to the formation of CoO−MgO solid solution. On the other hand, a better reducibility of CoO species has been reported upon Ni addition, and accounted for a decrease in their particle sizes.[22] This process may be initiated by formation of a solid solution of CoO and NiO, both exhibiting a rock salt-like structure. According to this proposal, it is a little puzzling why Ni acts as a diluent but Mg does not. For this reason, another process may be postulated, assuming that Ni^{2+} would substitute tetrahedral Co^{2+} in the Co_3O_4 spinel lattice. This would lead to $Co(Co_{2-x}Ni_x)O_4$ phases.[23] The broad peak of H_2 consumption at LT on Co−Ni−Mg−Al materials is very probably composed of two contributions (Figure 5), corresponding to the reduction of these phases in two steps. We previously pointed out the increase in reducibility of Co_3O_4 species with Co loading in Co−Ni−Mg−Al LDHs. A similar phenomenon has, in the case of Co/Al_2O_3, been assigned to a better nucleation process of the metallic nuclei.[24]

In the reduction processes in the HT domain (> 720 K) of the catalysts, several relevant features can be highlighted:

(1) The XRD patterns of the calcined Co- and Ni-rich samples exhibit characteristic lines of spinel and rock salt-like structures, respectively.

(2) Unlike in the LT domain, the reducibility of Co in samples in which Mg and/or Ni are present is higher than in Co(3)Al.

(3) Reduction of the spinel $CoAl_2O_4$ phase, giving rise to a straight and intense peak, was previously reported at least 100 K above the HT reduction peak of Co(3)Al.[13]

(4) Finally, the total H_2 consumption, not exceeding 1.17 [H_2/(Co+Ni)], shows that in multi-cationic samples the cations are not fully reduced. However, it is worth noting that the H_2 consumption relative to that observed for Co(3)Al, increases only slightly upon Mg addition, but more significantly upon Ni addition,.

We can tentatively estimate the H_2 consumption in the LT and HT domains for Co(3)Al, assuming that it would be decomposed into Co_3O_4 and $CoAl_2O_4$ spinel phases upon calcination at 773 K:

$$[Co_{0.75}Al_{0.25}(OH)_2][(CO_3^{2-})_{0.07}(NO_3^-)_{0.12}] \cdot 0.63\ H_2O \rightarrow 0.21\ Co_3O_4 + 0.125\ CoAl_2O_4 + 0.07\ CO_2 + 0.12\ NO + 1.63\ H_2O + 1.15\ O_2 \quad (1)$$

Theoretical H_2 consumption of 1.33 and 1 (H_2/Co) corresponds to the reduction of Co_3O_4 and $CoAl_2O_4$, respectively: close to the experimental values of 1.39 and 1.06 found when these phases are deposited on alumina.[13] This will result in H_2 consumption in the LT and HT domains of 1.11 and 0.17 for Co(3)Al. A large discrepancy is thus noted with the experimental values of 0.29 and 0.71 H_2/Co. Therefore, one should consider that Co_3O_4, reduced in the LT domain, exists in much lower quantities than would be expected from Equation (1). In contrast, a larger amount of a second phase more easily reducible than $CoAl_2O_4$ is formed in the HT domain; this phase might be Co_3AlO_6, as proposed by Arnoldy and Moulijn.[13] It could not be differentiated from $CoAl_2O_4$ by XRD, thanks to their similar patterns. When considering Co(2)Mg(1)Al, we might hypothesize that a $Co_{3-x}Mg_xAlO_6$ phase could probably exist.

When Co, Ni, Mg, and Al are present simultaneously, several phases are involved, because different mixed oxides and spinel-like structures could be formed. Anyway, the reduction profile is clearly modified when Ni content increases: i) the reduction starts at a lower temperature than in the Ni-free sample, ii) the peak becomes less asymmetric, with a progressive increase in intensity of the shoulder observed on the lower temperature side, iii) H_2 consumption increases. In contrast, the reducibility of Ni and Co seems almost insensitive to Mg content. However, as the reducibility of Co increases while that of Ni decreases with Mg content,[5] a compensating effect cannot be ruled out. Therefore, the presence of Ni(Mg)AlO- and $Co_{3-x-y}Ni_xMg_yAlO_6$-type phases can be postulated, with, of course, several other minor phases like, for example, alumina, depending of the nominal compositions of the samples.

To sum up: in Co−Ni−Mg−Al LDHs, the species reduced below 723 K (LT domain) would be a $Co_{3-x}Ni_xO_4$ mixed oxide with a spinel structure. Above 723 K (HT domain), mixed oxides of the NiMg(Al)O type, and a spinel phase containing both Co and Ni − tentatively assigned to $Co_{3-x-y}Ni_xMg_yAlO_6$ − can be proposed. The XRD pat-

tern has the aspect of the rock salt-like structure of the major NiMg(Al)O phase. The existence of a phase containing both Co and Ni is supported by recent results obtained in the hydrogenation of acetonitrile, in which the catalysts obtained from reduction of Co−Ni−Mg−Al LDHs were most active and selective for ethylamine than the catalysts prepared from Ni−Mg−Al and Co−Mg−Al LDHs.[3]

Conclusion

It was possible to obtain multi-component LDHs, accommodating Co, Ni, Mg, and Al cations in the same brucite-like sheet, without identifiable excess phase, in a wide range of compositions. The progressive substitution of Ni for Co decreases the lattice *a* parameter, inducing a stronger electrostatic attraction with the anions, the decomposition of which is thus shifted toward higher temperatures. The thermally decomposed samples are a mixture of Ni- and Mg-containing rock salt-type, and Co-containing spinel-like phases. Accordingly, the surface areas increase with the Ni or Mg content, accounting for the decreasing proportion of spinel-like phase in the mixture. The two distinct temperature domains observed in TPR are in agreement with the well known behavior of Co, giving spinel phases reduced below 720 K, while complex phases containing Co, Ni, and Mg are reduced above this temperature. The two maxima observed in the first domain and the enhancement of reducibility with Ni content suggest that a $Co_{3-x}Ni_xO_4$ phase is formed. H_2 consumption, shapes of the reduction profiles, and also XRD patterns make it plausible to propose that NiMg(Al)O and $Co_{3-x-y}Ni_xMg_yAlO_6$ phases are reduced above 720 K, in relative amounts depending on the stoichiometry of the LDHs. It is worth noting that the reducible Co and Ni cations are in close interaction in these phases, resulting in interesting properties when these materials are used as catalyst precursors.

Experimental Section

Preparation of the LDH Precursors: A solution containing the appropriate amounts of cobalt, nickel, magnesium, and aluminium nitrates (Aldrich) dissolved in 250 cm^3 of deionized water was delivered into a polypropylene reactor by a chromatography-type pump at a constant flow of 1 cm^3min^{-1} at room temperature and ambient atmosphere. A second aqueous solution of 1 M NaOH (SdS) was fed by a pH-stat apparatus (718 Stat Titrino, Metrohm) at a constant pH value of ca. 9.0 ± 0.2. After precipitation, the suspension was aged at 373 ± 5 K for 15 h with stirring. The solid product was isolated by centrifugation, washed thoroughly with deionized water, and dried overnight at 353 K in an oven. Nine samples were synthesized following this procedure, varying the ratio between the divalent cations and maintaining the ratio $M^{2+}/Al^{3+} \approx 3$ (Table 1).

These samples belong to two different families, with molar ratios in solution corresponding on the one hand to $Mg^{2+}/\Sigma M^{2+} = 1:3$ and variable $Ni^{2+}/\Sigma M^{2+}$ and, on the other hand to $Ni^{2+}/(Co^{2+}+Ni^{2+}) = 1:2$ and variable $Mg^{2+}/\Sigma M^{2+}$.

As an example, the multi-component Co−Ni−Mg−Al sample labeled Co(1.5)Ni(0.5)Mg(1)Al corresponds to a compound prepared from $M^{2+}/\Sigma M^{2+} = 1.5:3$, 0.5:3 and 1:3 for Co^{2+}, Ni^{2+}, and Mg^{2+}, respectively.

Characterization of the Solids: Chemical analyses of the samples were performed at the Service Central d'Analyse du C.N.R.S. (Solaize, France). Powder X-ray diffraction (XRD) patterns were recorded on a Philips instrument (40 kV, 20 mA) using Cu*K*α radiation (λ = 0.154 nm). The 2θ angle ranged from 6° to 70°. A monochromator was applied, to avoid fluorescence phenomena. Thermogravimetric experiments (TG) were carried out on a Setaram TG 85 1000 °C microbalance in air (80 cm^3min^{-1}) from 293 to 973 K (ramp: 2 K min^{-1}). Specific surface areas were determined by N_2 adsorption at 77 K with a Micromeritics ASAP 2000 instrument and using the BET equation. The samples were outgassed in vacuum ($2\cdot10^{-4}$ Pa) at 523 K overnight before N_2 adsorption. The calcination of the samples was carried out in an air flow at 573 or 773 K (ramp 2 K min^{-1}). The final temperature was maintained for 5 h.

The reducibility of the samples was examined by temperature programmed reduction by hydrogen (TPR). The experimental setup was derived from that proposed classically.[25] Detection was carried out with the thermal conductivity detector of a Shimadzu GC8 chromatograph. The experimental parameters were carefully selected to meet the recommendations of Monti and Baiker.[26] An aliquot of the catalyst (20−30 mg) was activated first at 623 K or 773 K for 4 h in air (ramp: 2 K min^{-1}, flow: 50 cm^3min^{-1}) and then cooled to room temperature. After flushing with He, the TPR was started in H_2/Ar gas (3:97 vol/vol, purity of both gases > 99.995%) from 293 to 1293 K (ramp: 10 K min^{-1}, flow: 20 cm^3min^{-1}).

[1] D. Tichit, A. Vaccari, *Appl. Clay Sc.* **1998**, *13*, 311−315.
[2] W. T. Reichle, *Chem. Technol.* **1986**, *16*, 58−63.
[3] B. Coq, D. Tichit, S. Ribet, *J. Catal.* **2000**, *189,* 117−128.
[4] F. Medina Cabello, D. Tichit, B. Coq, A. Vaccari, N. T. Dung, *J. Catal.* **1997**, *167*, 142−152.
[5] D. Tichit, F. Medina, B. Coq, R. Dutartre, *Appl. Catal. A: Gen.* **1997**, *159*, 241−258.
[6] S. Ribet, D. Tichit, B. Coq, B. Ducourant, F. Morato, *J. Solid State Chem.* **1999**, *142*, 382−392.
[7] S. Kannan, S. Velu, V. Ramkumar, C. S. Swamy, *J. Mater. Sci.* **1995**, *30*, 1462−1468.
[8] S. Kannan, A. Narayanan, C. S. Swamy, *J. Mater. Sci.* **1996**, *31*, 2353−2360.
[9] M. A. Ulibarri, J. M. Fernandez, F. M. Labajos, V. Rives, *Chem. Mater.* **1991**, *3*, 626−630.
[10] O. Clause, B. Rebours, E. Merlen, F. Trifiro, A. Vaccari, *J. Catal.* **1992**, *133*, 231−246.
[11] B. Rebours, J. B. d'Espinose de la Caillerie, O. Clause, *J. Am. Chem. Soc.* **1994**, *116*, 1707−1717.
[12] B. Basavalingu, J. A. K. Tareen, G. T. Bhandage, *J. Mater. Sci. Lett.* **1986**, *5*, 1227−1231.
[13] P. Arnoldy, J. A. Moulijn, *J. Catal.* **1985**, *93*, 38−54.
[14] F. Rouquerol, J. Rouquerol, K. Sing, *Adsorption by Powders & Porous Solids. Principles, Methodology and Applications*, Academic Press, London, **1999**.
[15] F. Trifiro, A. Vaccari, O. Clause, *Catal. Today* **1994**, *21*, 185−195.
[16] M. K. Titulaer, J. B. H. Jansen, J. W. Geus, *Clays Clay Min.* **1994**, *42*, 249−258.
[17] C. V. Rode, M. Arai, M. Shirai, Y. Nishiyama, *Appl. Catal. A: Gen.* **1997**, *148*, 405−413.
[18] H. Ming, B. C. Baker, *Appl. Catal. A: Gen.* **1995**, *123*, 23−36.
[19] M. K. Niemelä, A. O. I. Krause, *Catal. Lett.* **1995**, *34*, 75−84.

[20] E. Van Steen, G. S. Sewell, R. A. Makhothe, C. Micklethwaite, H. Manstein, M. de Lange, C. T. O'Connor, *J. Catal.* **1996**, *162*, 220−229.
[21] B. A. Sexton, A. E. Hughes, T. W. Turney, *J. Catal.* **1986**, *97*, 390−406.
[22] A. Y. Khodakov, J. Lynch, D. Bazin, B. Rebours, N. Zanier, B. Moisson, P. Chaumette, *J. Catal.* **1997**, *168*, 16−25.
[23] Y. E. Roginskaya, O. V. Morozova, E. N. Lubnin, Y. E. Ulitina, G. V. Lopukhova, S. Trasatti, *Langmuir* **1997**, *13*, 4621−4627.
[24] W. J. Wang, Y. W. Chen, *Appl. Catal. A: Gen.* **1991**, *77*, 223−233.
[25] J. L. Lemaitre, *Characterization of Heterogeneous Catalysts*, Marcel Dekker, New York, **1984**, p.34.
[26] D. A. M. Monti, A. Baiker, *J. Catal.* **1983**, *83*, 323−335.
Received March 3, 2000
[I00113]